

Synthesis and structure of a new three-dimensional indium phosphate with 16-membered one-dimensional channels †

A Thirumurugan and Srinivasan Natarajan*

Framework Solids Laboratory, Chemistry and Physics of Materials Unit,
Jawaharlal Nehru Centre for Advanced Scientific Research, Jakkur P.O., Bangalore 560 064,
India. E-mail: raj@jncasr.ac.in

Received 9th April 2003, Accepted 22nd July 2003

First published as an Advance Article on the web 28th July 2003

A new indium phosphate, $[\text{NH}_3(\text{CH}_2)_2\text{NH}_2(\text{CH}_2)_2\text{NH}_3]_2[\text{NH}_2(\text{CH}_2)_2\text{NH}_2(\text{CH}_2)_2\text{NH}_2][\text{In}_{6,8}\text{F}_8(\text{H}_2\text{O})_2(\text{PO}_4)_4(\text{HPO}_4)_4] \cdot 2\text{H}_2\text{O}$, **I**, has been prepared as a good single phase material employing hydrothermal methods using HF–pyridine as the solvent in the presence of diethylenetriamine (DETA). The structure is built-up from vertex linking $\text{InO}_4(\text{H}_2\text{O})_2$ and InO_4F_2 octahedral, and PO_4 and $\text{PO}_3(\text{OH})$ tetrahedral units, giving rise to a three-dimensional structure with large 16-membered one-dimensional channels. The organic amine along with water molecules occupies these channels. The formation of **I** with $\text{In} : \text{F} > 1$ and the presence of large channels are noteworthy features.

Introduction

Open-framework solids based on aluminosilicates and phosphates have been studied extensively during the last two decades, resulting in a large number of new materials with novel structures.^{1,2} Most of these compounds are made under hydrothermal conditions in the presence of organic amines. During the 1990s, the use of fluoride ions to the synthesis was observed to have a pronounced effect on the crystallization of many metal phosphates.^{3–5} In most cases, fluoride is incorporated as part of the framework giving rise to novel structures. Non-aqueous approaches, *i.e.*, replacing water with an alcohol, and the use of HF–pyridine as a solvent have helped in isolating compounds with new compositions.⁶ The use of HF–pyridine is particularly attractive as it gave rise to good quality siliceous ferrierite⁷ and many alumino-⁸ and gallophosphates.⁹ Though a large number of phosphates of Al and Ga have been prepared and characterized in great detail,^{2,5} work is slowly emerging on the synthesis of indium phosphates.^{10–17} During a course of a program of research aimed to prepare new solids with open-framework structures, we are now investigating the formation of indium phosphates employing HF–pyridine as the solvent. Our efforts gave rise to a new indium phosphate, $[\text{NH}_3(\text{CH}_2)_2\text{NH}_2(\text{CH}_2)_2\text{NH}_3]_2[\text{NH}_2(\text{CH}_2)_2\text{NH}_2(\text{CH}_2)_2\text{NH}_2][\text{In}_{6,8}\text{F}_8(\text{H}_2\text{O})_2(\text{PO}_4)_4(\text{HPO}_4)_4] \cdot 2\text{H}_2\text{O}$, **I**, with a three-dimensional structure possessing extra-large 16-membered channels. In this paper, we report the synthesis and structure of this compound.

Experimental

The title compound was synthesized hydrothermally using pyridine–HF as the solvent in the presence of diethylenetriamine (DETA). In a typical synthesis 0.335 g indium sulfate was dissolved in 1 ml of water. To this, 0.11 ml of phosphoric acid (85%), 0.12 ml of HF (48%) and 1.68 ml of pyridine were added under continuous stirring. Finally, 0.07 ml of DETA was added and the mixture was homogenized for 30 min at room temperature. The reaction mixture with the composition, $\text{In}_2(\text{SO}_4)_3 : 2.6\text{H}_3\text{PO}_4 : 5.2\text{HF} : 32.1\text{pyridine} : 0.88\text{DETA} : 85\text{H}_2\text{O}$, was transferred to a PTFE-lined stainless-steel pressure vessel (23 ml) and heated at 180 °C for 96 h under autogenous pressure. The initial pH of the reaction mixture was ~5 and the pH after the reaction was ~4. The resulting product, a crop of fine needle-shaped crystals, was filtered off, washed with water

and dried at room temperature (yield = 80% based on In). The product was characterized by powder XRD, TGA, IR and NMR studies.

The powder XRD pattern of **I** was collected using a STOE-STADI-P diffractometer with a monochromated Cu-K α X-ray source (step size of 0.03° and a collection time of 5 s per step, 2θ range = 3–50°). The XRD pattern indicated that the product is a new material; the pattern is entirely consistent with the structure determined by single-crystal X-ray diffraction. A least squares fit of the powder XRD (Cu-K α) lines, using the *hkl* indices generated from single-crystal X-ray data, gave the following cell: $a = 19.598(1)$, $b = 9.679(3)$, $c = 14.923(1)$ Å, $\beta = 118.9(4)^\circ$; which is in reasonable agreement with that determined by single crystal XRD. The experimental powder XRD pattern along with the simulated one is given in Fig. 1. Elemental analysis: found: N 6.01, C 6.88, H 2.64; calc.: N 6.04, C 6.91, H 2.83%.

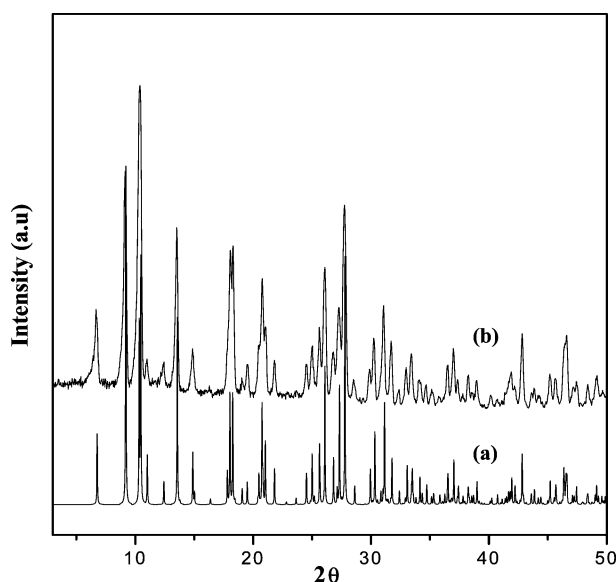


Fig. 1 Simulated (a) and experimental (b) powder X-ray (Cu-K α) diffraction (XRD) pattern for $[\text{NH}_3(\text{CH}_2)_2\text{NH}_2(\text{CH}_2)_2\text{NH}_3]_2[\text{NH}_2(\text{CH}_2)_2\text{NH}_2(\text{CH}_2)_2\text{NH}_2][\text{In}_{6,8}\text{F}_8(\text{H}_2\text{O})_2(\text{PO}_4)_4(\text{HPO}_4)_4] \cdot 2\text{H}_2\text{O}$, **I**.

Thermogravimetric analysis (TGA) was carried out in oxygen atmosphere (flow rate = 50 ml min⁻¹) in the range between 25 and 700 °C (heating rate = 10 °C min⁻¹). The compound showed a gradual initial weight loss followed by a sharp loss around 350 °C (ESI †). The total weight loss of 17.3% corresponds well

† Electronic supplementary information (ESI) available: TGA analysis and ¹H decoupled ³¹P MAS NMR spectrum for **I**. See <http://www.rsc.org/suppdata/dt/b3/b303998f>

Table 1 Crystal data and structure refinement parameters for $[\text{NH}_3(\text{CH}_2)_2\text{NH}_2(\text{CH}_2)_2\text{NH}_3]_2[\text{NH}_2(\text{CH}_2)_2\text{NH}_2(\text{CH}_2)_2\text{NH}_2][\text{In}_{6.8}\text{F}_8(\text{H}_2\text{O})_2(\text{PO}_4)_4(\text{HPO}_4)_4]\cdot 2\text{H}_2\text{O}, \mathbf{I}$

Empirical formula	$\text{C}_3\text{N}_{2.25}\text{H}_{9.50}\text{In}_{1.70}\text{P}_2\text{F}_2\text{O}_9$
Formula mass	515.83
Crystal system	Monoclinic
Space group	$C2/m$ (no. 12)
$a/\text{\AA}$	19.569(5)
$b/\text{\AA}$	9.7034(18)
$c/\text{\AA}$	14.927(6)
$\beta/^\circ$	119.091(14)
$V/\text{\AA}^3$	2476.9(12)
Z	8
T/K	293(2)
$D_s/\text{g cm}^{-3}$	2.748
μ/mm^{-1}	3.600
Independent reflections	1897 ($R_{\text{int}} = 0.0278$)
R Indexes [$I > 2\sigma(I)$]	$R_1 = 0.0274$, $wR_2 = 0.0695^b$

$^a R_1 = \sum ||F_o| - |F_c|| / \sum |F_o|$. $^b wR_2 = \{\sum [w(F_o^2 - F_c^2)]^2 / \sum [w(F_o^2)]\}^{1/2}$; $w = 1/[\sigma^2(F_o) + (aP)^2 + bP]$, $P = [\text{max.}(F_o^2, 0) + 2(F_c^2)]/3$, where $a = 0.0354$ and $b = 11.6285$.

with the loss of water and amine molecules (calc. 16.9%). The calcined product was poorly crystalline, as indicated by broad powder XRD lines, and corresponds to the crystalline phase InPO_4 (JCPDS: 8-0052). Infrared (IR) spectra were recorded in the range 400–4000 cm^{-1} using the KBr pellet method. The IR spectra showed the expected typical peaks; IR bands for **I**: lattice water: 3581, 1610 cm^{-1} , $\nu(\text{NH})$: 1514 cm^{-1} , $\nu(\text{CN})$: 1096, 1051 cm^{-1} , $\nu(\text{CH})$: 3195, 3081 cm^{-1} , $\nu(\text{P-OH})$: 1047 cm^{-1} , $\delta(\text{P-OH})$: 1460 cm^{-1} .

Single crystal structure determination

A suitable colorless single crystal was carefully selected under a polarizing microscope and glued to a thin glass fiber with cyanoacrylate (superglue) adhesive. Crystal structure determination by X-ray diffraction was performed on a Siemens SMART-CCD diffractometer equipped with a normal focus, 2.4 kW sealed tube X-ray source (Mo- $K\alpha$ radiation, $\lambda = 0.71073$ \AA) operating at 40 kV and 40 mA. A hemisphere of intensity data were collected at room temperature in 1321 frames with ω scans (width of 0.30° and exposure time of 20 s per frame) in the 2θ range 3–46.5°. Pertinent experimental details for the structure determination are presented in Table 1.

An absorption correction based on symmetry equivalent reflections was applied using the SADABS program.¹⁸ The structure was solved by direct methods, which readily revealed a sufficient fragment of the structure (In, P and O) to enable the remainder of the non-hydrogen atoms to be located from difference Fourier maps and the refinements to proceed to $R < 10\%$. One of the In atoms, In(5) was found to have a refined site occupancy of only 0.196, though occupying a special position. Most of the hydrogen positions, especially those belonging to the framework and one of the amine molecules, were located in the difference map and for the final refinement the hydrogen atoms were placed in geometrically idealized positions and held in the riding mode. All the hydrogen position of the other amine molecule could not be located in the difference Fourier map, possibly due to disorder at the central nitrogen position, and hence no hydrogen positions were included in the final refinement. In addition, soft geometrical constraints for the C(3) and C(4) distances were employed for this amine molecule, to keep the molecule intact. The last cycles of refinement included atomic positions for all the atoms, anisotropic thermal parameters for all non-hydrogen framework atoms, and isotropic thermal parameters for all the hydrogen atoms. Full-matrix least-squares refinement against $|F^2|$ was carried out using the SHELXTL-PLUS¹⁹ suite of programs. Details of the final refinement are given in Table 1. Selected bond distances and angles are given in Table 2.

CCDC reference number 204105.

See <http://www.rsc.org/suppdata/dt/b3/b303998f/> for crystallographic data in CIF or other electronic format.

Results and discussion

The structure is based on the vertex linking of $\text{InO}_4(\text{H}_2\text{O})_2$ and InO_4F_2 octahedral, and PO_4 and $\text{PO}_3(\text{OH})$ tetrahedral units giving rise to a three-dimensional structure. The asymmetric unit contains five independent indium and two phosphorus atoms (Fig. 2). All the indium atoms occupy special positions and the P atoms have general positions. Thus, In(1) and In(2) lie in the mirror planes (m), while In(3), In(4) and In(5) occupy the $2/m$ sites. The fluorine atoms, F(1), F(4), F(6) and F(7) along with the oxygen atoms, O(4) and O(11) also lie on the mirror planes. All the indium atoms are octahedrally coordinated to four oxygen and two fluorine atoms, except In(5) which is coordinated only by oxygen atoms. The In–O/F bond distances are in the range 2.061(4)–2.165(4) \AA and O/F–In–O/F bond angles are in the range 79.9(2)–180°. While In(1) possess two terminal fluorine atoms [F(1) and F(4)], In(2), In(3) and In(4) are connected through F(6) and F(7) atoms. Of the two phosphorus atoms, P(2) has four P–O–In bonds, and P(1) has three such connections and possesses one terminal P–O linkage [P(1)–O(13)]. The P–O bond distances are in the range 1.498(4)–1.541(6) \AA and the average O–P–O bond angle is 109.4°. Bond valence sum calculations for **I** based on the method of Brown and Altermatt,²⁰ using $r_o(\text{In-F}) = 1.792$ \AA and $r_o(\text{In-O}) = 1.902$ \AA , indicated that the valence sums are in the expected range for the participating ions and are listed in Table 2. The partial occupancy of In(5) atoms, in **I**, appears to result in a nominally anionic framework. The excess negative charge on the framework, however, may be balanced by the protonation of the terminal nitrogen atoms of the second organic amine molecule, the hydrogen atoms of which were not located in the difference Fourier maps. Similar behavior of differential protonation of amine molecules has been encountered before.²¹

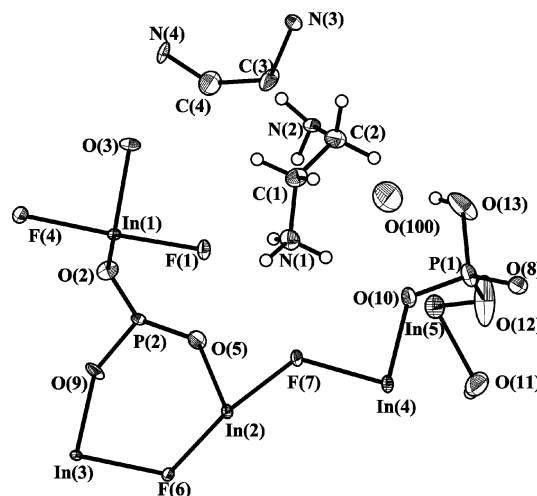


Fig. 2 ORTEP diagram of **I**. Thermal ellipsoids are given at 30% probability.

The complex octahedral–tetrahedral framework structure of **I** can be understood by considering simpler building blocks. Thus, In(2), In(3) and In(4) octahedra are linked through their fluorine vertex forming an infinite one-dimensional In–F–In chains. P(1) and P(2) tetrahedra are grafted on to this chain giving rise to an arrangement reminiscent of the structure of tancoite.²² $\text{In(5)O}_4(\text{H}_2\text{O})_2$ octahedra link these tancoite-like chains through P(1)O₃(OH) forming a layer in the bc plane as shown in Fig. 3. Thus, the layer consists of a tancoite chain and a one-dimensional corner-shared chain formed by P(1), In(5)

Table 2 Selected bond lengths (Å) and angles (°) in $[\text{NH}_3(\text{CH}_2)_2\text{NH}_2(\text{CH}_2)_2\text{NH}_3]_2[\text{NH}_2(\text{CH}_2)_2\text{NH}_2(\text{CH}_2)_2\text{NH}_2] [\text{In}_{6,8}\text{F}_8(\text{H}_2\text{O})_2(\text{PO}_4)_4(\text{HPO}_4)_4] \cdot 2\text{H}_2\text{O}$, I. Values in square brackets are the bond valences. Their sum (SVB) appears in bold type at the end of the list of the distances for each cation

In(1)–F(1)	2.062(4) [0.483]	In(4)–F(7)	2.114(4) [0.420]
In(1)–O(2)#1	2.094(4) [0.595]	In(4)–O(10)	2.116(4) [0.561]
In(1)–O(2)	2.094(4) [0.595]	In(4)–O(10)#2	2.116(4) [0.561]
In(1)–O(3)	2.129(4) [0.541]	In(4)–O(10)#3	2.116(4) [0.561]
In(1)–O(3)#1	2.129(4) [0.541]	In(4)–O(10)#1	2.116(4) [0.561]
In(1)–F(4)	2.164(5) [0.365]	$\Sigma(\text{In}–\text{O}/\text{F})$	[3.084]
$\Sigma(\text{In}–\text{O}/\text{F})$	[3.12]		
In(2)–O(5)#1	2.093(4) [0.595]	In(5)–O(11)	2.003(7) [0.763]
In(2)–O(5)	2.093(4) [0.595]	In(5)–O(11)#6	2.003(7) [0.763]
In(2)–F(6)	2.101(4) [0.433]	In(5)–O(12)#7	2.187(5) [0.462]
In(2)–F(7)	2.122(4) [0.408]	In(5)–O(12)	2.187(5) [0.462]
In(2)–O(8)#2	2.130(4) [0.539]	In(5)–O(12)#6	2.187(5) [0.462]
In(2)–O(8)#3	2.130(4) [0.539]	In(5)–O(12)#3	2.187(5) [0.462]
$\Sigma(\text{In}–\text{O}/\text{F})$	[3.11]	$\Sigma(\text{In}–\text{O})$	[3.37]^a
In(3)–O(9)	2.088(4) [0.605]	P(1)–O(8)	1.500(4) [1.379]
In(3)–O(9)#4	2.088(4) [0.605]	P(1)–O(10)	1.505(4) [1.350]
In(3)–O(9)#5	2.088(4) [0.605]	P(1)–O(12)	1.514(6) [1.325]
In(3)–O(9)#1	2.088(4) [0.605]	P(1)–O(13)	1.534(6) [1.228]
In(3)–F(6)#4	2.116(4) [0.417]	$\Sigma(\text{P}–\text{O})$	[5.28]
In(3)–F(6)	2.116(4) [0.417]		
$\Sigma(\text{In}–\text{O}/\text{F})$	[3.25]		
In(4)–F(7)#2	2.114(4) [0.420]	P(2)–O(5)	1.519(4) [1.303]
		P(2)–O(2)	1.520(4) [1.293]
		P(2)–O(9)	1.528(4) [1.272]
		P(2)–O(3)#8	1.539(4) [1.231]
		$\Sigma(\text{P}–\text{O})$	[5.099]
F(1)–In(1)–O(2)#1	99.11(15)	F(7)#2–In(4)–O(10)#2	85.54(14)
F(1)–In(1)–O(2)	99.12(15)	F(7)–In(4)–O(10)#2	94.46(14)
O(2)#1–In(1)–O(2)	86.5(2)	O(10)–In(4)–O(10)#2	180.0
F(1)–In(1)–O(3)	92.56(15)	F(7)#2–In(4)–O(10)#3	85.54(13)
O(2)#1–In(1)–O(3)	167.71(16)	F(7)–In(4)–O(10)#3	94.46(13)
O(2)–In(1)–O(3)	95.55(16)	O(10)–In(4)–O(10)#3	93.2(2)
F(1)–In(1)–O(3)#1	92.52(15)	O(10)#2–In(4)–O(10)#3	86.8(2)
O(2)#1–In(1)–O(3)#1	95.57(16)	F(7)#2–In(4)–O(10)#1	94.46(13)
O(2)–In(1)–O(3)#1	167.70(16)	F(7)–In(4)–O(10)#1	85.54(13)
O(3)–In(1)–O(3)#1	79.9(2)	O(10)–In(4)–O(10)#1	86.8(2)
F(1)–In(1)–F(4)	177.70(17)	O(10)#2–In(4)–O(10)#1	93.2(2)
O(2)#1–In(1)–F(4)	82.53(14)	O(10)#3–In(4)–O(10)#1	179.998(2)
O(2)–In(1)–F(4)	82.53(14)	O(11)–In(5)–O(11)#6	179.998(1)
O(3)–In(1)–F(4)	85.72(14)	O(11)–In(5)–O(12)#7	90.1(3)
O(3)#1–In(1)–F(4)	85.72(14)	O(11)#6–In(5)–O(12)#7	89.9(3)
O(5)#1–In(2)–O(5)	90.9(3)	O(11)–In(5)–O(12)	90.1(3)
O(5)#1–In(2)–F(6)	94.62(14)	O(11)#6–In(5)–O(12)	89.9(3)
O(5)–In(2)–F(6)	94.62(14)	O(12)#7–In(5)–O(12)	81.2(3)
O(5)#1–In(2)–F(7)	91.44(14)	O(11)–In(5)–O(12)#6	89.9(3)
O(5)–In(2)–F(7)	91.44(14)	O(11)#6–In(5)–O(12)#6	90.1(3)
F(6)–In(2)–F(7)	171.35(16)	O(12)#7–In(5)–O(12)#6	98.8(3)
O(5)#1–In(2)–O(8)#2	87.33(19)	O(12)–In(5)–O(12)#6	179.999(1)
O(5)–In(2)–O(8)#2	177.92(18)	O(11)–In(5)–O(12)#3	89.9(3)
F(6)–In(2)–O(8)#2	86.68(13)	O(11)#6–In(5)–O(12)#3	90.1(3)
F(7)–In(2)–O(8)#2	87.44(14)	O(12)#7–In(5)–O(12)#3	180.0
O(5)#1–In(2)–O(8)#3	177.92(18)	O(12)–In(5)–O(12)#3	98.8(3)
O(5)–In(2)–O(8)#3	87.33(19)	O(12)#6–In(5)–O(12)#3	81.2(3)
F(6)–In(2)–O(8)#3	86.68(13)	O(8)–P(1)–O(10)	113.4(3)
F(7)–In(2)–O(8)#3	87.44(14)	O(8)–P(1)–O(12)	112.3(3)
O(8)#2–In(2)–O(8)#3	94.4(3)	O(10)–P(1)–O(12)	110.1(3)
O(9)–In(3)–O(9)#4	180.0	O(8)–P(1)–O(13)	106.7(3)
O(9)–In(3)–O(9)#5	87.7(3)	O(10)–P(1)–O(13)	105.0(4)
O(9)#4–In(3)–O(9)#5	92.3(3)	O(12)–P(1)–O(13)	108.9(5)
O(9)–In(3)–O(9)#1	92.3(3)	O(5)–P(2)–O(2)	112.4(2)
O(9)#4–In(3)–O(9)#1	87.7(3)	O(5)–P(2)–O(9)	111.9(2)
O(9)#5–In(3)–O(9)#1	180.00(19)	O(2)–P(2)–O(9)	108.7(3)
O(9)–In(3)–F(6)#4	87.36(14)	O(5)–P(2)–O(3)#8	108.6(3)
O(9)#4–In(3)–F(6)#4	92.64(14)	O(2)–P(2)–O(3)#8	108.4(2)
O(9)#5–In(3)–F(6)#4	92.64(14)	O(9)–P(2)–O(3)#8	106.6(2)
O(9)#1–In(3)–F(6)#4	87.36(14)	P(2)–O(2)–In(1)	137.4(3)
O(9)–In(3)–F(6)	92.64(14)	P(2)#8–O(3)–In(1)	130.7(2)
O(9)#4–In(3)–F(6)	87.36(14)	P(2)–O(5)–In(2)	137.3(3)
O(9)#5–In(3)–F(6)	87.36(14)	In(2)–F(6)–In(3)	122.27(19)
O(9)#1–In(3)–F(6)	92.64(14)	In(4)–F(7)–In(2)	126.4(2)
F(6)#4–In(3)–F(6)	180.0	P(1)–O(8)–In(2)#2	137.5(3)
F(7)#2–In(4)–F(7)	179.998(1)	P(2)–O(9)–In(3)	139.1(3)
F(7)#2–In(4)–O(10)	94.46(14)	P(1)–O(10)–In(4)	127.0(2)
F(7)–In(4)–O(10)	85.54(14)	P(1)–O(12)–In(5)	132.3(4)

Symmetry transformations used to generate equivalent atoms: #1 $x, -y - 1, z$; #2 $-x + 1, -y - 1, -z - 1$; #3 $-x + 1, y, -z - 1$; #4 $-x + 1, -y - 1, -z$; #5 $-x + 1, y, -z$; #6 $-x + 1, -y, -z - 1$; #7 $x, -y, z$; #8 $-x + 3/2, -y - 1/2, -z$; #8 $-x + 3/2, -y - 1/2, -z$.^a The In(5) atom has a refined SOF of 0.196 (occupying the 2/m site: SOF = 0.25).

Table 3 Important hydrogen bond interactions in $[\text{NH}_3(\text{CH}_2)_2\text{NH}_2(\text{CH}_2)_2\text{NH}_3]_2[\text{NH}_2(\text{CH}_2)_2\text{NH}_2(\text{CH}_2)_2\text{NH}_2][\text{In}_{6.8}\text{F}_8(\text{H}_2\text{O})_2(\text{PO}_4)_4(\text{HPO}_4)_4]\cdot 2\text{H}_2\text{O}$, **I**

D—H ⋯ A	D—H/Å	H ⋯ A/Å	D—A/Å	D—H ⋯ A/°
N(1)—H(1) ⋯ F(1)	0.89	2.01	2.776(6)	143
N(1)—H(2) ⋯ O(10)	0.89	2.34	3.131(7)	149
N(1)—H(3) ⋯ F(4)#1	0.89	2.04	2.892(6)	161
N(2)—H(8) ⋯ F(4)#1	0.90	1.80	2.693(1)	175
N(3)—H(10) ⋯ O(12)#2	0.89	2.24	2.967(8)	139
N(3)—H(11) ⋯ O(3)#3	0.89	2.19	2.910(8)	138
O(11)—H(30) ⋯ O(13) ^a #4	0.82	2.28	3.107(1)	160
C(2)—H(6) ⋯ O(13)	0.97	2.41	3.303(1)	152

Symmetry operations used to generate equivalent atoms: #1 $3/2 - x, 1/2 + y, -z$; #2 $3/2 - x, -1/2 - y, -1 - z$; #3 $2 - x, -1 - y, -z$; #4 $1 - x, -y, -1 - z$. ^a Intra-framework.

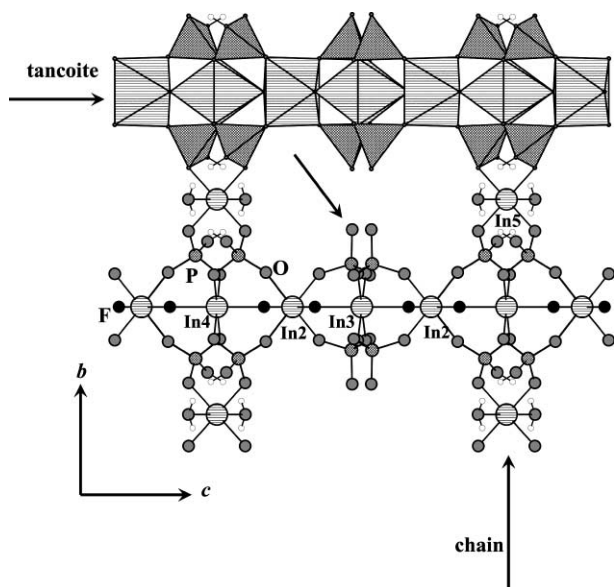


Fig. 3 Structure of **I** in the *bc* plane showing the tancoite chain and the one-dimensional corner-shared chain within the layer structure. The arrow indicates the position where In(1) (not shown) links with the layer to give rise to the three-dimensional structure (see text).

and In(4) polyhedra. In(1)O₄F₂ octahedra cross-link the layers forming the three-dimensional structure with extra-large 16-membered channels along the *b* axis (Fig. 4). The protonated diethylenetriamine molecule along with water molecules occupy these channels. The presence of terminal fluoride, water, along with —OH groups, gives rise to large number of hydrogen bond

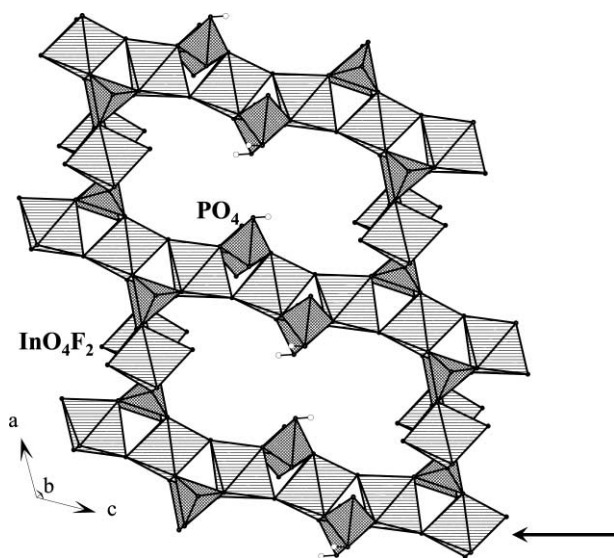


Fig. 4 Structure of **I** in the *ac* plane showing the extra-large 16-membered channels. Arrow indicates the tancoite chains. Amine and water molecules are not shown for clarity.

interactions involving the amine and extra-framework water molecules. The N ⋯ F and N ⋯ O distances are in the range 2.688(2)–2.988(2) and 2.903(1)–3.132(1) Å with a large number of N—H ⋯ F/O angles (~150°). Important hydrogen bond interactions are listed in Table 3.

NMR experiments were performed on a Bruker DSX 300 MHz with resonance frequencies of 121 MHz for ³¹P. Magic angle spinning (MAS) was performed at a rotating frequency of 7 kHz using a 4.0 mm rotor system. The spectra were referenced relative to H₃PO₄ (85 wt%) for ³¹P. The proton decoupled ³¹P pulsed MAS NMR spectra were recorded with a pulse width of 4.75 μs and a total of 1000 scans were collected with a recycle time of 1 s. The spectrum indicates the presence of two phosphorus sites, one as a shoulder with chemical shifts δ_{iso} = -1.745 ppm and δ_{iso} = 5.849 ppm (ESI †).

Though the literature is abound with reports of aluminium (ALPOs) and gallium phosphates (GAPOs), the number of indium phosphates are very few. It is likely that the larger size of In compared to Al and Ga could be one of the important factors. The larger size of indium necessitates a change from the classical all-tetrahedral frameworks found for many ALPOs and aluminosilicate zeolites, to higher ones. In this respect, the use of a large excess of fluorine in the synthesis mixture can help the formation of phosphate frameworks for larger sized metals by coordination to surplus metal sites. This would allow polyhedral connectivities between the metals through the bridging F atoms, as found for **I**.

In addition, **I** is a rare example where the F : In ratio is greater than unity and in which the F atoms are coordinated with both terminal and bridging environments. A similar fluorine rich indium phosphate [NH₃(CH₂)₃NH₃]₄[3H₃O][In₉F₁₆(HPO₄)₂(PO₄)₆]₃·3H₂O, possessing three-dimensional structure, has been reported recently.¹⁶ It is likely that the use of excess HF in the reaction medium resulted in frameworks possessing more fluorine than the metal. The fluorine atoms in these compounds occupy bridging positions and allow the formation of In—F—In chains, which also results in the indium octahedra to bond together giving rise to the tancoite chains. The presence of tancoite chains within a three-dimensional structure, to our knowledge, has not been observed before, though such instances have been observed in two-dimensional structures.²³

The pillaring of layers by InO₄F₂ in **I** is somewhat similar to that observed in the indium phosphate [C₃N₂H₅]₃[In₈(HPO₄)₁₄(H₂O)₆]₃·5H₂O(H₃O), reported by Chippindale *et al.*,¹² which also possess 16-membered channels. A 14-membered channel structure with HPO₄ pillared layers, [NH₃(CH₂)₃NH₃]₄[3H₃O][In₉F₁₆(HPO₄)₂(PO₄)₆]₃·3H₂O, has also been reported.¹⁶ In **I**, the tancoite chains are connected through a corner-shared chain forming a layer and are pillared by InO₄F₂ units.

In conclusion, the synthesis and structure of a three-dimensional octahedral–tetrahedral indium phosphate with extra-large 16-membered one-dimensional channels has been accomplished. We believe the use of HF–pyridine may lead to more diverse structural types for octahedral–tetrahedral framework materials. Additionally, the large excess of F⁻ ions

in the reaction would allow the formation of framework structures with unusual stoichiometries and structures not observed in other alumino- and gallophosphate materials. We are currently pursuing this theme.

Acknowledgements

S. N. thanks the Council of Scientific and Industrial Research (CSIR), Govt. of India, for the award of a research grant and A. T. for the award of a research fellowship.

References

- 1 R. M. Barrer, *Hydrothermal Chemistry of Zeolites*, Academic Press, London, 1982.
- 2 A. K. Cheetham, T. Loiseau and G. Ferey, *Angew. Chem., Int. Ed.*, 1999, **38**, 3268, and references therein.
- 3 J. L. Guth, H. Kessler and R. Wey, *Stud. Surf. Sci. Catal.*, 1991, **60**, 63.
- 4 A. Merrouche, J. Patarin, H. Kessler, M. Soulard, L. Delmotte, J. L. Guth and F. Joly, *Zeolites*, 1992, **12**, 226.
- 5 G. Ferey, *J. Fluorine Chem.*, 1995, **72**, 187.
- 6 S. Feng and R. R. Xu, *Acc. Chem. Res.*, 2001, **34**, 239.
- 7 S. J. Weigel, J. C. Gabriel, E. G. Puebla, M. A. Bravo, N. J. Henson, L. M. Bull and A. K. Cheetham, *J. Am. Chem. Soc.*, 1996, **118**, 2427.
- 8 A. Kuperman, S. Nadimi, S. Oliver, G. A. Ozin, J. M. Garces and M. M. Olken, *Nature*, 1993, **365**, 239.
- 9 R. E. Morris and S. J. Weigel, *Chem. Soc. Rev.*, 1997, **26**, 309.
- 10 S. C. Dhingra and R. C. Haushalter, *J. Chem. Soc., Chem. Commun.*, 1993, 1665; S. C. Dhingra and R. C. Haushalter, *J. Solid State Chem.*, 1994, **112**, 96.
- 11 Y. Xu, L. L. Koh, L. H. An, R. R. Xu and S. L. Qiu, *J. Solid State Chem.*, 1995, **117**, 373.
- 12 A. M. Chippindale, S. J. Brech, A. R. Cowley and W. M. Simpson, *Chem. Mater.*, 1996, **8**, 2259.
- 13 A. M. Chippindale and S. J. Brech, *Chem. Commun.*, 1996, 2781.
- 14 K.-H. Lii and Y.-F. Huang, *Inorg. Chem.*, 1999, **38**, 1348.
- 15 H. Du, J. Chen, W. Pang, J. Yu and I. D. Williams, *Chem. Commun.*, 1997, 781.
- 16 I. D. Williams, J. Yu, H. Di, J. Chen and W. Pang, *Chem. Mater.*, 1998, **10**, 773.
- 17 M. P. Attfield, A. K. Cheetham and S. Natarajan, *Mater. Res. Bull.*, 2000, **35**, 1007.
- 18 G. M. Sheldrick, SADABS Simens Area Detector Absorption Correction Program, University of Göttingen, Germany, 1994.
- 19 G. M. Sheldrick, SHELXTL-PLUS Program for Crystal Structure Solution and Refinement, Bruker AXS Inc., Madison, WI, USA, 1996.
- 20 I. D. Brown and D. Altermatt, *Acta Crystallogr., Sect. B*, 1985, **41**, 244.
- 21 S. Mandal, S. Natarajan, J. M. Greneche, M. Riou-Cavellec and G. Ferey, *Chem. Mater.*, 2002, **14**, 3751–3757.
- 22 F. C. Hawthorne, *Acta Crystallogr., Sect. B*, 1994, **50**, 481, and references therein.
- 23 S. Chakrabarti and S. Natarajan, *Angew. Chem., Int. Ed.*, 2002, **41**, 1224.